Brazilian Journal of Chemical Engineering

ISSN 0104-6632
Printed in Brazil
www.abeq.org.br/bjche

Vol. 33, No. 03, pp. 491 - 501, July - September, 2016
dx.doi.org/10.1590/0104-6632.20160333s20150128

TRANSITION PHENOMENON INVESTIGATION BETWEEN DIFFERENT FLOW REGIMES IN A ROTARY DRUM

D. A. Santos, R. Scatena, C. R. Duarte and M. A. S. Barrozo*

Universidade Federal de Uberlândia, Faculdade de Engenharia Química, Building K,
Campus Santa Mônica, 38400-902, Uberlândia - MG, Brazil.
Fax: (55) (34) 32394188
E-mail: masbarrozo@ufu.br

(Submitted: February 26, 2015 ; Revised: June 1, 2015 ; Accepted: June 4, 2015)

Abstract - Rotary drums can show different granular flow regimes each one with its own specific flow behavior, which increase the complexity in their study. The way particles move inside the rotary drum is directly related to the mass and energy transfer rates, and consequently to the process performance. Thus, an experimental investigation regarding the transition between different flow regimes inside a rotary drum was carried out in the present work. To the best of our knowledge, the hysteresis phenomenon was observed for the first time in the transition between cataracting-centrifuging regimes, which was shown to be dependent on the physical properties of the particles such as sphericity, density and particle-wall friction coefficient. A new expression for the centrifuging critical rotation speed was proposed in this work.
Keywords: Critical rotation speed; Particle shape; Froude number.

INTRODUCTION

Many industrial processes use rotating drums in several applications, such as mixing, granulation, milling, coating and drying (Fernandes *et al*., 2009; Arruda *et al*., 2009a; Lobato *et al*. 2008; Arruda *et al*., 2009b; Lisboa *et al*. 2007). As a result, the fluid dynamic behaviour in rotating drums has attracted numerous research efforts from both the engineering and physics communities over the past few decades (Silvério *et al*., 2011; Santos *et al*. 2015).

Depending on some of the geometric dimensions (drum diameter and length), operating conditions (filling degree and rotation speed), and particle properties (size, shape and friction characteristics), the bed material inside rotary drums can flow in different ways (sliding, slumping, rolling, cascading, cataracting and centrifuging regimes). The slumping, rolling and cascading regimes are the most used regimes in industrial processes, e.g., mixing, granulation, drying and coating, while the cataracting regime is mainly used in milling processes. On the other hand, the sliding and centrifuging regimes are not used at all and must be avoided (Henein *et al*., 1983; Mellmann, 2001; Santomaso *et al*., 2003).

Most of these flow regimes have been studied (Boateng and Barr, 1997; Ding *et al*., 2001; Ding *et al*., 2002; Chou *et al*., 2010; Yada *et al*., 2010; Huang *et al*., 2012; Chou and Hsiau, 2012; Demagh *et al*., 2012; Santos *et al*., 2013; Dubé *et al*., 2013; Lee *et al*., 2013), although there are a restricted number of works dedicated to the transition phenomenon between the regimes (Henein *et al*., 1983a,b; Watanabe, 1999; Mellmann, 2001; Santomaso *et al*., 2003; Juarez *et al*., 2011).

Very low rotation speeds combined with a smooth drum wall can induce the sliding and slumping regimes to occur. The sliding regime is characterized

*To whom correspondence should be addressed
This is an extended version of the work presented at the 20th Brazilian Congress of Chemical Engineering, COBEQ-2014, Florianópolis, Brazil.

by a static bed of material perfectly sliding adjacent to the drum wall with no particle mixing. As the drum rotation speed or the wall roughness increases, the slumping regime appears as a combination of upward and downward solid movements. In this regime the material moves as a rigid body, reaching an upper angle of repose and then sliding down or avalanching until a lower angle of repose is established. At higher rotation speeds, the transition to the rolling regime takes place. This regime presents a nearly flat surface with a constant inclination, characterizing the dynamic angle of repose of the material.

With further speed increments, an "S" shaped curve develops at the bed surface corresponding to the cascading regime. For even higher rotation speeds, the cataracting regime is observed, since particles are projected from the surface into the air space (Blumberg and Schlünder, 1996; Mellmann, 2001; Liu *et al*., 2005; Juarez *et al*., 2011).

According to Watanabe (1999) the critical rotation speed for centrifuging can be defined in two different ways: the critical rotation speed is reached when the particles are pushed against the drum wall, forming a ring all together (Figure 1(a)); otherwise, when just the outermost layer of the bed material forms a ring, the critical rotation speed is achieved (Figure 1(b)).

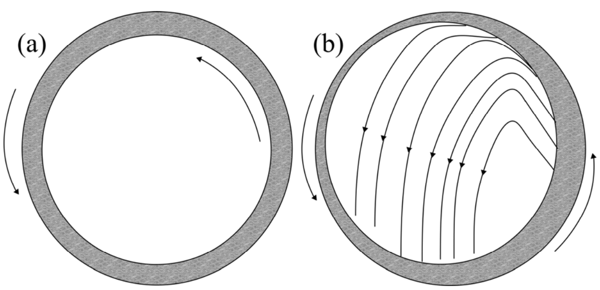

Figure 1: Different definitions for centrifuging transition: (a) the particles form a ring all together; (b) just the outermost layer of the bed material forms a ring.

As claimed by Blumberg and Schlünder (1996), a quantitative analysis of the flow regime transition boundaries can be assessed by using the Froude number (F_r). The Froude number, $F_r=\omega^2 R/g$, is defined as the ratio of centrifugal force to gravity, where ω, R and g are the drum rotation speed, drum radius and the gravitational acceleration, respectively.

Based on the centrifuging definition depicted in Figure 1(a), some specific relationships have been developed, over the last few decades, in order to forecast the cataracting-centrifuging transition (Table 1).

Table 1: Different models for the cataracting-centrifuging transition prediction.

Classical mechanics	
$\omega_C = \sqrt{\frac{g}{R}}$	(1)
Rose and Sullivan (1957)	
$\omega_C = \sqrt{\frac{2g}{2R-2r}}$	(2)
Walton and Braun (1993)	
$\omega_C = \sqrt{\frac{g}{R\sin\theta_S}}$	(3)
Ristow (1998)	
$\omega_C = \sqrt{\frac{g}{R\sqrt{1-f}}}$	(4)
Watanabe (1999)	
$\omega_C = \sqrt{\frac{g}{R\sin\theta_S\sqrt{1-f}}}$	(5)
Juarez *et al*. (2011)	
$\omega_C = \sqrt{\frac{g\left(1-\rho_f/\rho_S\right)}{R\sin\theta_S\sqrt{1-f}}}$	(6)

In classical mechanics, the equilibrium of forces is achieved when the Froude number is equal to one and the corresponding rotation speed is well known as the critical rotation speed for centrifuging (ω_c) (Equation (1)). Efforts have been concentrated on the consideration of particle physical properties and geometric effects in the cataracting-centrifuging boundary position modeling (Equations (2)-(5)), where r, θ_S and f are the particle radius, the angle of repose and the filling degree, respectively.

Juarez *et al*. (2011) studied the effect of particle diameter, filling degree and interstitial fluid on the critical rotation speed for centrifuging in a quasi-2D rotary drum by means of experiments and numerical simulations. Based on experiments in liquid granular systems, the authors proposed an expression for the critical rotation speed, where ρ_f and ρ_S are the densities of the fluid and solid phases, respectively (Equation (6)).

Although some expressions for the critical rotation speed have been proposed, the transition phenomenon between the different regimes, mainly to the centrifuging regime, has not yet been systematically examined. Additionally, since the industrial process efficiency depends on the granular flow regime established under given operating conditions of the rotary drum, the ability to predict the particle motion inside this equipment, including the particle properties effect, is of primary importance.

So, the present work is dedicated to an understanding of how the critical rotation speed is related to the material properties, such as particle shape, density and diameter.

EXPERIMENTAL SETUP

For the particle dynamics study, a batch rotary drum composed of a cylindrical part made of stainless steel with a 0.22 m inner diameter and 0.50 m in length was used. To enable the cross-section observation of the granular flow, a glass front wall was adopted. The following flow regimes were investigated in the present work: rolling, cascading, cataracting and centrifuging (Figure 2).

In order to avoid the occurrence of the sliding regime, a suitable sandpaper (P80) was glued to the inside wall of the drum. The critical rotation speeds for the transition between the regimes were determined as a function of the filling degree varying from 0.1 to 0.6 stepped by 0.05.

It is worth noting that, in this work we considered, as a criterion for the cataracting-centrifuging transition, the case where just the outermost layer of the bed material forms a ring (Figure 2(d)).

Five different granular materials were used: rice, corn, tablet (placebo tablets with a concave cylindrical shape), soybean and glass beads. The material densities were measured by means of a Micromeritics AccuPyc 1331 gas pycnometer. For the particle size characterization, the volume based particle size (D_V), which is defined as the diameter of an equivalent sphere having the same volume as a given particle, was adopted.

With regards to the determination of particle sphericity, dynamic digital images were analyzed for each granular material using the CAMSIZER® dynamic image analysis system, which allows the storage and processing of a large number of projected images at various measurement angles (Figure 3) (Cardoso *et al*., 2013).

After image analysis Equation (7) was used for sphericity (ϕ) calculation, where d_{CI} and d_{CC} are the inscribed and the circumscribed circle diameters, respectively (Peçanha and Massarani, 1980):

$$\phi = \frac{d_{CI}}{d_{CC}} \tag{7}$$

The particle-wall friction coefficient was determined by lifting an inclined plane covered with the same material as the inside drum wall (sandpaper P80) with free particles on it. When the particles started rolling down the plane, the plane inclined angle (β) was used for the particle-wall friction coefficient ($\mu_{p\text{-}w}$) calculation (Equation (8)):

$$\mu_{p-w} = \tan(\beta) \tag{8}$$

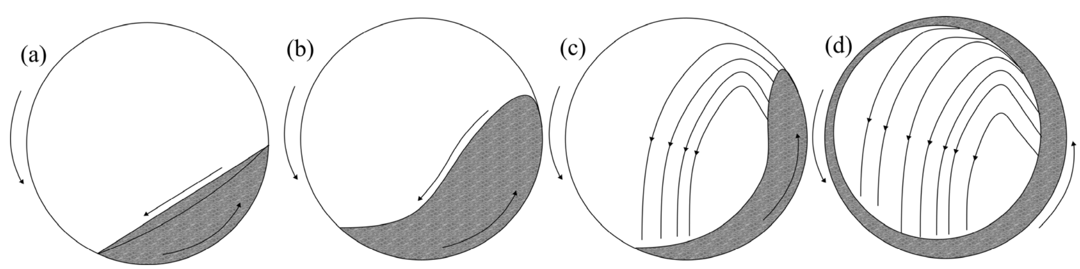

Figure 2: Transverse bed motions in a rotary drum investigated in the present work: (a) rolling regime; (b) cascading regime; (c) cataracting regime; (d) centrifuging regime.

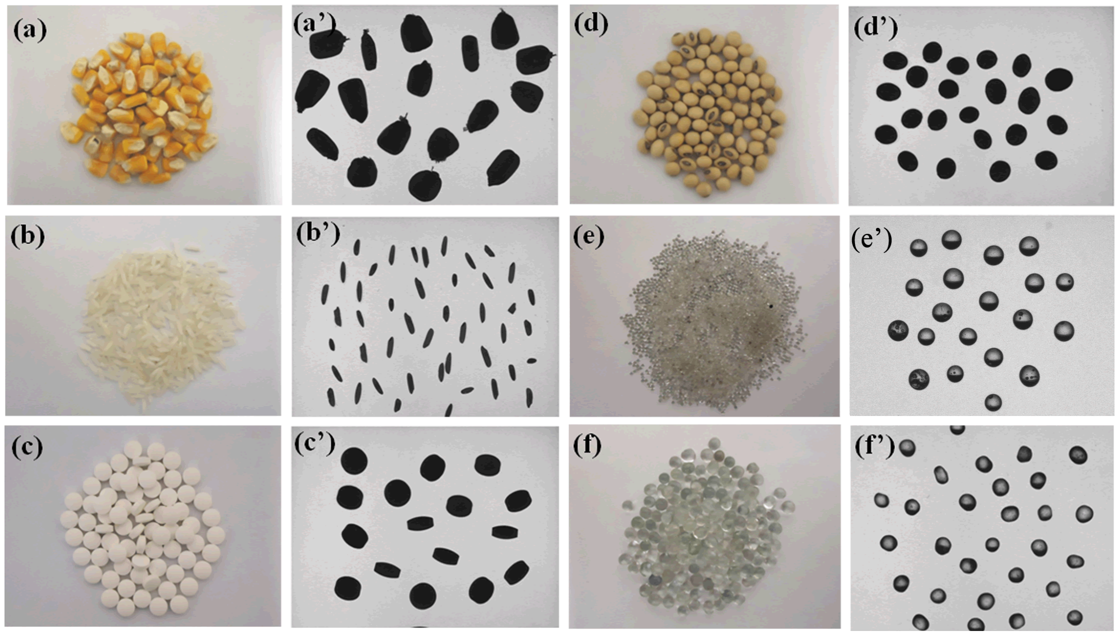

Figure 3: Different materials used in the present investigation along with the respective projected shadows processed by means of the CAMSIZER® analysis system: (a) corn; (b) rice; (c) tablet (placebo tablets with a concave cylindrical shape); (d) soybean; (e) glass bead A; (f) glass bead B.

RESULTS AND DISCUSSION

In order to investigate the effect of particle characteristics on the transition flow regime phenomenon observed in a rotary drum, different types of granular materials were used whose physical properties are shown in Table 2, where ρ_S, D_V, ϕ and $\mu_{p\text{-}w}$ are the solid density, volume based particle size, sphericity, and particle-wall friction coefficient, respectively. These granular materials have been used in several applications (Barrozo *et al*. 1996; Santos *et al*., 2012; Ribeiro *et al*. 2005; Silva *et al*. 2011; Oliveira *et al*. 2009).

Table 2: The main physical properties of the used granular materials.

Materials	ρ_S [kg/m³]	D_V [m]	ϕ [-]	$\mu_{p\text{-}w}$ [-]
Tablet	1517	0.00662	0.50	0.90
Corn	1288	0.00788	0.66	0.76
Rice	1465	0.00277	0.35	0.73
Soybean	1164	0.00639	0.84	0.31
Glass bead A	2460	0.00113	0.91	0.48
Glass bead B	2460	0.00422	0.86	0.35

It can be observed, by means of Table 2, that the particle-wall friction coefficient ($\mu_{p\text{-}w}$) is higher for irregular particles (lower values of ϕ) compared to round particles (higher values of ϕ), which can be attributed to the fact that irregular particles have higher surface contact area and their rotations are therefore more suppressed, as would be expected.

All of the transition curves were determined visually, using a high speed video camera, by both gradually increasing the rotation speed (increasing curve), from the rolling regime until the centrifuging regime, and gradually decreasing the rotation speed (decreasing curve), from the centrifuging regime until the rolling regime, as a function of the filling degree.

Investigation of the Rolling-Cascading Flow Regime Transition

For the rolling-cascading transition, Blumberg and Schlünder (1996) observed, by means of experiments carried out using two different drum diameters (0.1 m and 0.29 m), and different particle diameters (0.55-5.0 mm), a strong dependence of the drum rotation speed required for cascading on the particle size (Equation (9)):

$$F_{rc} \approx \frac{2d}{D} \tag{9}$$

where F_{rc}, D and d are the critical Froude number for cascading, the inner drum diameter and the particle diameter, respectively (Blumberg and Schlünder, 1996).

Due to lack of validation of Equation (9) for different types of particles, Figure 4 presents a comparison between experimental rolling-cascading transition curves, measured in the present work using different materials, and the predicted values using the Blumberg and Schlünder (1996) equation (Equation (9)). Since no significant differences were observed between the increasing and decreasing curves for cascading regardless of the material used, just the experimental increasing curves were plotted in Figure 4.

It can be seen that the effect of filling degree on the rolling-cascading transition, observed experimentally, is not taken into consideration in Equation (9). Generally speaking, the best agreement between experiment and the predictions of Equation (9) were obtained when using round particles (higher values of ϕ), since Equation (9) was originally developed using spherical particles of aluminium silicate.

In spite of typical critical Froude number ranges for the rolling regime condition being reported in the literature, e.g. $10^{-4} < F_r < 10^{-2}$ (Mellmann, 2001) and $5\text{x}10^{-4} < F_r < 2\text{x}10^{-2}$ (Henein *et al.*, 1983), the particle shape effect should be considered besides the rotational speed and particle diameter, in order to better represent the rolling-cascading transition phenomenon. So, we suggest the replacement of the diameter (d) in Equation (9) by the volume equivalent diameter (D_V) multiplied by the sphericity (ϕ) (Equation (10)):

$$F_{rc} \approx \frac{2D_V\phi}{D} \tag{10}$$

The results obtained using Equation (10) are also presented in Figure 4 in comparison with those determined by means of Equation (9). Table 3 shows the critical Froude number relative errors calculated as averages over the filling degree range.

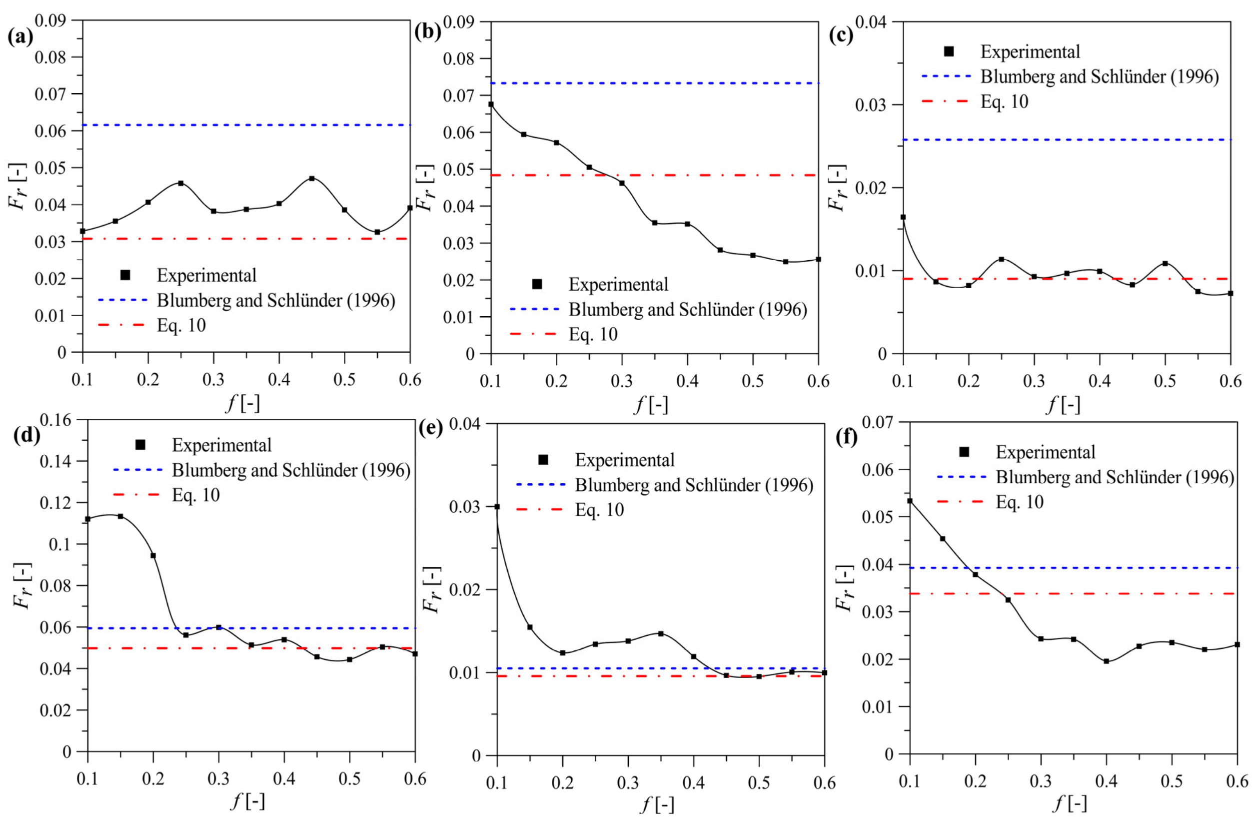

Figure 4: Transition curves between rolling-cascading regimes: (a) tablet; (b) corn; (c) rice; (d) soybean; (e) glass bead A; (f) glass bead B.

Table 3: Relative average error between Equation (9) and Equation (10) in the critical Froude number prediction for cascading.

Materials	Eq. (9) mean percentage error (%)	Eq. (10) mean percentage error (%)
Rice	176.31	15.20
Tablet	59.71	20.14
Corn	99.53	43.83
Soybean	24.66	20.51
Glass bead A	20.68	23.07
Glass bead B	52.29	38.02

It should be noted that the errors using Equation (9) were larger than those using Equation (10), mainly for irregular particles. Despite of the improvement given by Equation (10) in the rolling-cascading transition prediction, including round and irregular particles, further investigation concerning the filling degree effect is required.

Investigation of The Cataracting-Centrifuging Flow Regime Transition

Regarding the cataracting-centrifuging transition, Watanabe (1999) and Mellmann (2001) observed that the critical rotation speed for centrifuging significantly depends on the filling degree, since lower values of filling degrees require a very high rotation speed ($F_{rc} > 1$) in order to centrifuge.

Since the critical Froude number for centrifuging (F_{rc}) approaches, approximately, to a value of unity asymptotically as the filling degree (f) increases, the authors of the present work propose the following expression for the cataracting-centrifuging transition:

$$F_{rc} = 1 + \lambda \exp(-\tau f) \tag{11}$$

Substituting $F_{rc} = \omega_c^2 R/g$ into Equation (11) and solving for the critical rotation speed (ω_c), results in:

$$\omega_c = \sqrt{\frac{g\left[1 + \lambda \exp\left(-\tau f\right)\right]}{R}} \tag{12}$$

It can be noted, by means of Equation (12), that depending on the value of τ as $f \rightarrow 1$ the term $\lambda\exp(-\tau f) \rightarrow 0$ and, consequently, Equation (12) reduces to Equation (1) ($F_{rc} = 1$), which corresponds to the theoretical force equilibrium. On the other hand, as f decreases ($f \rightarrow 0$), the critical rotation speed for centrifuging increases ($F_{rc} > 1$), which is in accordance with experimental observations (Watanabe, 1999; Mellmann, 2001).

So, λ is the additional effect of the Froude number necessary for the centrifuging transition when using low values of filling degrees and τ is related to the exponential decay of critical rotation speed for centrifuging (ω_c) with filling degree (f) during the cataracting-centrifuging transition. Both parameters are expected to be dependent on the physical characteristics of the particle.

Figure 5 shows the experimental cataracting-centrifuging transition curves (critical Froude number plotted against filling degree) in a rotary drum, using different granular materials, along with the corresponding fitted curves using Equation (11).

It can be seen that the critical rotation speeds for centrifuging, in the case of decreasing rotation speed (closed squares), were different from that in the case of increasing rotation speed (closed triangles), and the effect was more pronounced for round particles (higher values of ϕ) at lower values of filling degrees. Therefore, for the first time, the hysteresis phenomenon was observed, in the transition between the cataracting-centrifuging regimes.

The hysteresis was strongly influenced by the particle shape, which can be attributed to the fact that for round particles, where the contact area between particle-wall and particle-particle is significantly reduced to a near single point, the transfer of momentum is more inefficient when compared to irregular particles. Additionally, irregular particles can form stable structures upstream, which facilitate particles sticking to the drum wall. Thus, the cataracting-centrifuging transition boundaries occur, in the case of increasing curves, at much higher rotational speeds for round particles than for irregular particles.

In the present investigation, the parameters λ and τ from Equation (11) for both the centrifuging increasing curve (λ_I and τ_I) and centrifuging decreasing curve (λ_D and τ_D) were adjusted for different granular materials (Figure 5), by means of a nonlinear regression (Table 4).

The correlation coefficients were above 0.96 for all the cases, showing an exponential trend between critical Froude number for centrifuging (F_{rc}) and filling degree (f).

As can be observed in Table 4, the materials were divided into two different groups, called here Group 1 and Group 2. Group 1 was composed of particles with lower values of λ and τ (irregular particles) while the materials that presented higher values of parameters λ and τ (rounded particles) were put into Group 2. Significant differences can be observed between the flow of round particles and that of irregular particles.

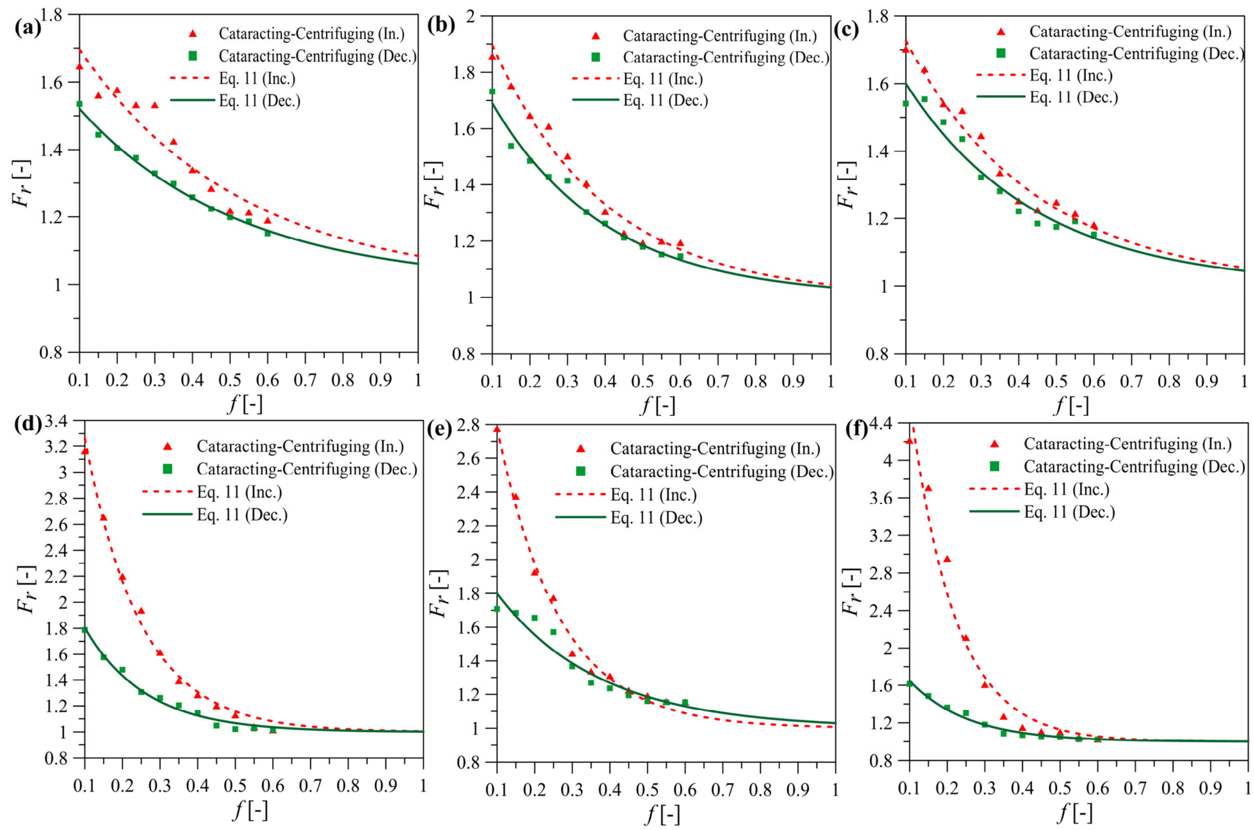

Figure 5: Transition curves between cataracting-centrifuging regimes: (a) tablet; (b) corn; (c) rice; (d) soybean; (e) glass bead A; (f) glass bead B.

Table 4: The adjusted λ and τ parameters by means of a nonlinear regression using Equation (11).

Materials		Increasing Curve		Decreasing Curve	
		λ_I	τ_I	λ_D	τ_D
Group 1	Tablet	0.88	2.34	0.66	2.37
	Corn	1.25	3.33	0.96	3.30
	Rice	0.97	2.89	0.80	2.88
Group 2	Soybean	4.40	6.66	1.49	6.18
	Glass bead A	3.24	6.00	1.15	3.64
	Glass bead B	8.38	8.35	1.23	6.44

It can be noted that all of the irregular particles (Group 1) showed no significant differences between λ_I and λ_D and between τ_I and τ_D, which means that, for this class of particles, the increasing and the decreasing curves for centrifuging were quite similar and, consequently, the hysteresis was less pronounced.

On the other hand, round particles (Group 2), which were characterized by lower values of particle-wall friction coefficient ($\mu_{p\text{-}w}$) and higher values of sphericity (ϕ), were strongly affected by the hysteresis phenomenon ($\lambda_I \neq \lambda_D$ and $\tau_I \neq \tau_D$) (see Table 4 and Figure 5).

The effect of particle size on the cataracting-centrifuging transition can be assessed by comparing glass bead A and glass bead B. It can be seen that, for a constant density, the hysteresis is more accentuated for the particle having the greater diameter.

It is also worth noting that, for all the materials that belong to Group 1, the averages of the parameters λ and τ (including increasing and decreasing curve values) were 0.92 and 2.85 and the standard deviations were 0.19 and 0.43, respectively. This effort represents an attempt to generalize the cataracting-centrifuging transition expression for this class of particles, although additional experiments using other materials should be carried out in order to confirm these findings.

To further investigate the particle shape effect on the granular flow transition, dynamic angles of repose were measured for the current materials as a function of filling degree (f) and drum rotation speed (ω) (Figure 6).

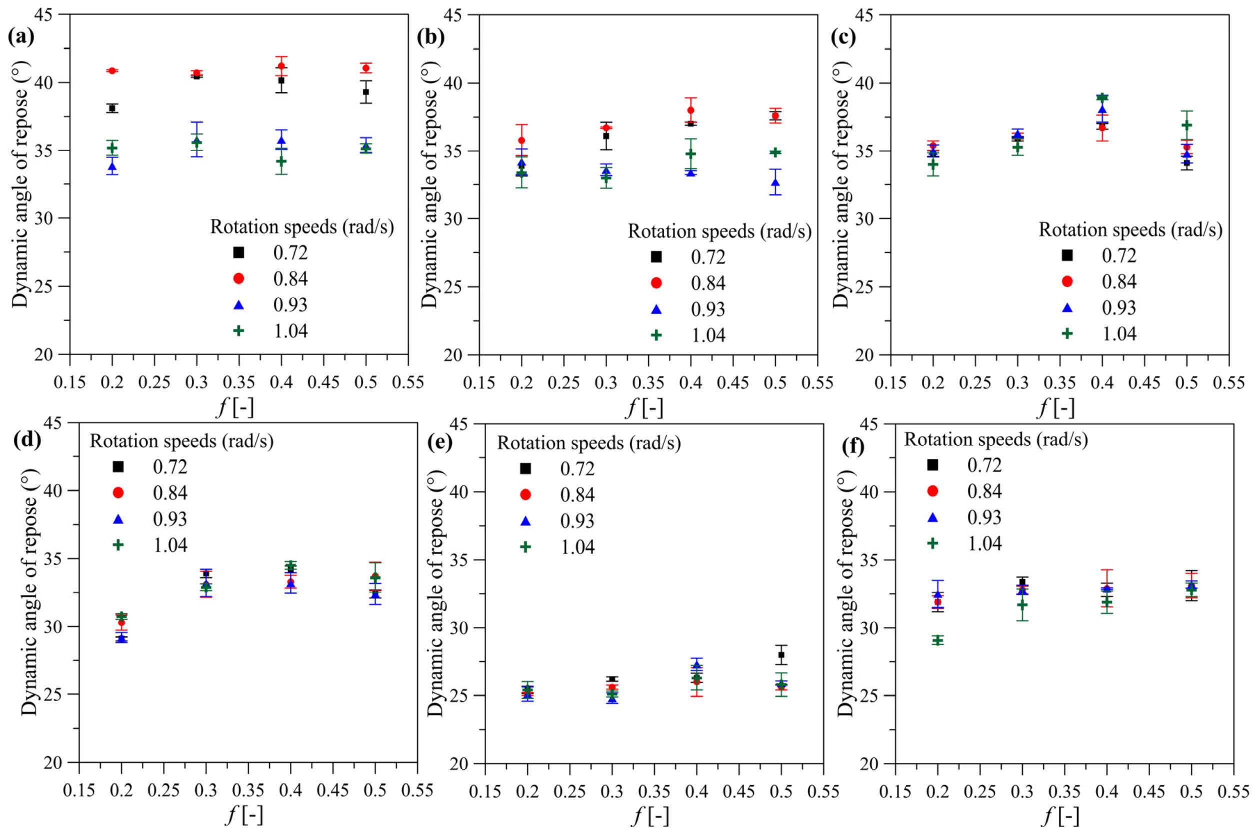

Figure 6: The measured dynamic angle of repose as a function of rotational speed and filling degree: (a) tablet; (b) corn; (c) rice; (d) soybean; (e) glass bead A; (f) glass bead B.

The present drum rotation speed range was chosen in the dynamic angles of repose measurements in order to guarantee the rolling regime condition for all the materials ($0.006 < F_r < 0.01$).

Figure 6 shows that the use of particles from Group 1 resulted in significantly higher dynamic angles of repose when compared to the respective values using particles from Group 2. As also observed by Dubé *et al*. (2013), instead of rolling, a different packing mechanism takes place, which enables the interlocking of irregular particles and, consequently, the construction of a particle bed skeleton near the drum wall, thus yielding higher dynamic angles of repose.

So, the dynamic angle of repose, which is related to the particle shape and roughness, provides a suitable guide to the cataracting-centrifuging transition phenomenon since the higher the particle dynamic angle of repose the lower the critical rotation speed for centrifuging and, consequently, the lower the hysteresis effects.

It is also interesting to note that, within the experimental error, the measured dynamic angles of repose using the materials from Group 1 were more dependent on drum rotational speed than on filling degree and this dependence tends to decrease as the particle-wall friction coefficient (μ_{p-w}) decreases (Figures 6(a), (b) and (c)). On the other hand, for the materials from Group 2 (Figures 6(d), (e) and (f)), the dynamic angles of repose were more influenced by the filling degree than by the drum rotation speed, which makes the influence of particle shape on the flow dynamics inside a rotary drum evident.

CONCLUSIONS

- Based on experiments carried out in a rotary drum over a wide range of rotation speed and filling degree and using different granular materials, it was possible to investigate the transition phenomenon between different flow regimes, whose main conclusions are as follows:
- The rolling regime is the most commonly operated flow regime in industry and the majority of

industrial granular materials differ significantly from round particles. Although a correlation for the rolling-cascading transition has been proposed by Blumberg and Schlünder (1996), this model fails to predict the granular flow involving irregular particles. Thus, a modification of the Blumberg and Schlünder model equation for the rolling-cascading transition was proposed by the introduction of the particle shape effect, represented here by the sphericity. In spite of the improvement given by this model in the rolling-cascading transition prediction, including round and irregular particles, further investigation concerning the filling degree effect is required;

- For the first time, the hysteresis phenomenon was observed in the transition between cataracting-centrifuging regimes, which was shown to be dependent on the physical properties of the particles such as sphericity, density and particle-wall friction coefficient;
- Design and operating decisions regarding the majority of processes performed in rotary drums are routinely made based on a fixed theoretical critical rotational speed, without a fundamental understanding of the transition phenomenon. For instance, in fertilizer granulation processes, independent of the filling degree and particle properties, the rotational speed is usually fixed between 25% and 40% of the critical speed beyond which centrifugation occurs. In this sense, a new expression relating the critical rotation speed for centrifuging as a function of the filling degree, which takes into consideration the particle properties and the hysteresis effects, was proposed by the present authors;
- The higher the particle dynamic angle of repose, which is related to the particle shape and roughness, the lower the critical rotation speed for centrifuging and, consequently, the lower the hysteresis effects;
- Additional experiments, using other materials such as fertilizer (used in granulation processes), different tablet shapes (used in coating processes), cylindrical polyethylene pellets (used in plastics manufacturing processes) etc., should be carried out in order to confirm these findings.

ACKNOWLEDGMENT

The authors are grateful to the State of Minas Gerais Research Support Foundation (FAPEMIG), the National Council for Scientific and Technological Development (CNPq) and Coordination for the Improvement of Higher Education Personnel (CAPES) for their financial support.

LIST OF SYMBOLS

d_{CI}	inscribed circle diameter [m]
d_{CC}	circumscribed circle diameter [m]
d	particle diameter [m]
D_V	volume based particle size [m]
f	filling degree [-]
F_r	Froude number [-]
F_{rc}	critical Froude number for flow regimes transition [-]
g	gravity acceleration [m.s^{-2}]
R	drum radius [m]

Greek Symbols

β	angle of inclination used in the particle-wall friction coefficient measurement [°]
θ_S	angle of repose of the material [°]
λ	parameter of Eq. (11) [-]
λ_I	parameter of Eq. (11) for increasing curve [-]
λ_D	parameter of Eq. (11) for decreasing curve [-]
μ_{p-w}	particle-wall friction coefficient [-]
ρ_f	fluid density [kg.m^{-3}]
ρ_S	solid density [kg.m^{-3}]
τ	parameter of Eq. (11) [-]
τ_I	parameter of Eq. (11) for increasing curve [-]
τ_D	parameter of Eq. (11) for decreasing curve [-]
ω	drum rotation speed [s^{-1}]
ω_c	critical rotation speed for centrifuging [s^{-1}]
ϕ	sphericity [-]

REFERENCES

Arruda, E. B., Lobato, F. S., Assis, A. J., Barrozo, M. A. S., Modelling of fertilizer drying in roto-aerated and conventional rotary dryers. Drying Technol., 27, 1192-1198 (2009a).

Arruda, E. B., Façanha, J. M. F., Pires, L. N., Assis, A. J., Barrozo, M. A. S., Conventional and modified rotary dryer: Comparison of performance in fertilizer drying. Chemical Eng. Proc., 48, 1414-1418 (2009b).

Barrozo, M. A. S., Sartori, D. J. M., Freire, J. T., Achcar, J. A., Discrimination of equilibrium moisture equations for soybean using nonlinearity measures. Drying Technol., 14, 1779-11794 (1996).

Blumberg, W., Schlünder, E.-U., Transversale Schüttgutbewegung und konvektiver Stoffübergang in Drehrohren. Teil 1: Ohne Hubschaufeln.

Chemical Engeniiring Proc., 35, 395-404 (1996). (In German).

Boateng, A. A., Barr, P. V., Granular flow behaviour in the transverse plane of a partially filled rotating cylinder. J. Fluid Mech., 330, 233-249 (1997).

Cardoso, C. R., Oliveira, T. J. P., Santana Junior, J. A., Ataíde, C. H., Physical characterization of sweet sorghum bagasse, tobacco residue, soy hull and fiber sorghum bagasse particles: Density, particle size and shape distributions. Powder Technol., 245, 105-114 (2013).

Chou, S. H., Hsiau, S. S., Dynamic properties of immersed granular matter in different flow regimes in a rotating drum. Powder Technol., 226, 99-106 (2012).

Chou, S. H., Liao, C. C., Hsiau, S. S., An experimental study on the effect of liquid content and viscosity on particle segregation in a rotating drum. Powder Technol., 201, 266-272 (2010).

Demagh, Y., Moussa, H. B., Lachi, M., Noui, S., Bordja, L., Surface particle motions in rotating cylinders: Validation and similarity for an industrial scale kiln. Powder Technol., 224, 260-272 (2012).

Ding, Y. L., Forster, R., Seville, J. P. K., Parker, D. J., Granular motion in rotating drums: Bed turnover time and slumping–rolling transition. Powder Technol., 124, 18-27 (2002).

Ding, Y. L., Forster, R., Seville, J. P. K., Parker, D. J., Segregation of granular flow in the transverse plane of a rolling mode rotating drum. Int. J. Multiphase Flow, 28, 635-663 (2002).

Ding, Y. L., Seville, J. P. K., Forster, R., Parker, D. J., Solids motion in rolling mode rotating drums operated at low to medium rotational speeds. Chem. Eng. Sci., 56, 1769-1780 (2001).

Dubé, O., Alizadeh, E., Chaouki, J., Bertrand, F., Dynamics of non-spherical particles in a rotating drum. Chem. Eng. Sci., 101, 486-502 (2013).

Fernandes, N. J., Ataide, C. H., Barrozo, M. A. S, Modeling and experimental study of hydrodynamic and drying characteristics of an industrial rotary dryer. Braz. J. Chem. Eng., 26, 331-341 (2009).

Henein, H., Brimacombe, J. K., Watkinson, A. P., Experimental studies of transverse bed motion in rotary kilns. Metallurgy Trans., B, 14, 191-205 (1983a).

Henein H, Brimacombe, J. K., Watkinson, A. P., The modelling of transverse solids motion in rotary kilns. Metallurgy Trans., B, 14, 207-220 (1983b).

Huang, A. N., Kuo, H. P., A study of the three-dimensional particle size segregation structure in a rotating drum. AIChE J., 58, 1076-1083 (2012).

Juarez, G., Chen, P., Lueptow, R. M., Transition to centrifuging granular flow in rotating tumblers: A modified Froude number. New Journal of Physics, 13, 1-12 (2011).

Lee, C.-F., Chou, H.-T., Capart, H., Granular segregation in narrow rotational drums with different wall roughness: Symmetrical and asymmetrical patterns. Powder Technol., 233, 103-115 (2013).

Liu, X. Y., Spechta, E., Mellmann, J., Experimental study of the lower and upper angles of repose of granular materials in rotating drums. Powder Technol., 154, 125-131 (2005).

Lisboa, M. H., Vitorino, D. S., Delaiba, W. B., Finzer, J. R. D., Barrozo, M. A. S., A study of particle motion in rotary dryer. Braz. J. Chem. Eng., 24(3), 265-374 (2007).

Lobato, F. S., Steffen, V., Arruda, E. B., Barrozo, M. A. S., Estimation of drying parameters in rotary dryers using differential evolution. J. Phys. Conf. Series, 135, 1-8 (2008).

Mellmann, J., The transverse motion of solids in rotating cylinders-forms of motion and transition behavior. Powder Technol., 118, 251-270 (2001).

Oliveira, D. C., Almeida, C. A. K., Vieira, L. G. M., Damasceno, J. J. R., Barrozo, M. A. S., Influence of geometrical dimensions on the behavior of a filtering hydrocyclone: an experimental and numerical study. Braz. J. Chem. Eng., 26, 575-582 (2009)

Peçanha, R. P., Massarani, G., Avaliação do desempenho de hidrociclones. Revista Brasileira de Tecnologia, Rio de Janeiro, 11, 289-299 (1980). (In Portuguese).

Rajchenbach, J., Flow in Powders: From discrete avalanches to continuous regime. Phys. Rev. Lett., 65, 2221-2224 (1990).

Ribeiro, J. A., Oliveira D. T., Passos, M. L., Barrozo, M. A. S., The use of nonlinearity measures to discriminate the equilibrium moisture equations for *Bixa orellana* seeds, J. Food Eng., 66, 63-68. (2005).

Ristow, G. H., Flow properties of granular materials in three-dimensional geometries. Habilitationsschrift, Philipps-Universität Marburg, 63-92 (1998).

Rose, H. E., Sullivan, R. M. E., A Treatise on the Internal Mechanics of Ball, Tube and Rod Mills. Constable, London, 35-68 (1957).

Santomaso, A. C., Ding, Y. L., Lickiss, J. R., York, D. W., Investigation of the granular behaviour in a rotating drum operated over a wide range of rotational speed. IChemE, 81, 936-945 (2003).

Santos, K. G., Santos, D. A., Duarte, C. R., Murata, V. V., Barrozo, M. A. S., Spouting of bidisperse mixture of particles: A CFD and experimental study. Drying Technol., 30, 1354-1367 (2012).

Santos, D. A., Petri, I. J., Duarte, C. R., Barrozo, M. A. S., Experimental and CFD study of the hydrodynamic behavior in a rotating drum. Powder Technol., 250, 52-62 (2013).

Santos, D. A., Dadalto, F. O., Scatena, R., Duarte, C. R., Barrozo, M. A. S., A hydrodynamic analysis of a rotating drum operating in the rolling regime. Chem. Eng. Res. Des., 94, 204-212 (2015).

Silva, D. O., Tamiozzo, L. M., Duarte, C. R., Murata, V. V., Barrozo, M. A. S., Modeling of seed coating in a spouted bed. Drying Technol., 29, 286-294 (2011).

Silvério, B. C., Façanha, J. M. F., Arruda, E. B., Murata, V. V., Barrozo, M. A. S., Fluid dynamics in concurrent rotary dryer and comparison of their performance with a modified dryer. Chem. Eng. Technol., 34, 81-86 (2011).

Walton, O. R., Braun R. L., Simulation of rotary-drum and repose tests for frictional spheres and rigid sphere clusters. Proc. Joint DOE/NFS Workshop on Flow of Particulates and Fluids, 1-18 (1993).

Watanabe, H., Critical rotation speed for ball-milling. Powder Technol., 104, 95-99 (1999).

Yada, H., Kawaguchi, T., Tanaka, T., Relation between segregation patterns and granular flow modes in conical rotating drum. Flow Meas. Instrum., 21, 207-211 (2010).